

3D dopant analysis in nano scale devices (FinFETs) by Atom Probe Tomography

Ajay Kumar Kambham^{1,2}, Arul Kumar^{1,2}, Wilfried Vandervorst^{1,2}

¹IMEC, Kapeldreef 75, B-3001 Leuven, ²K.U.Leuven, Department of Physics and Astronomy, B-3001, Leuven, Belgium

Corresponding author: klajaykumar@gmail.com

Abstract: The performance of nano scale devices depends on the detailed dopant distribution. Moving towards 3D-structures like FinFETs, studying the dopant gate overlap and conformality of doping calls for metrology with 3D-resolution and the ability to confine the analyzed volume to a small 3D-structure. We demonstrate such a methodology using Atom probe tomography (APT) for 3D-dopant profiling in FinFETs with nm-spatial resolution and demonstrate that APT is providing information on the 3D-dopant distribution in Fin devices required to understand the device performance. We demonstrate that the APT results are entirely consistent with observed device performances (I_{off} vs. I_{on}).

Key words: 3D-dopant distribution, FinFET, Conformality, Gate overlap, Atom probe tomography.

Introduction: The introduction of 3D devices like FinFETs for the sub-22nm nodes brings a challenge for doping profile formation and optimization. The optimization of dopant distribution in FinFET based devices can be performed by traditional ion implantation (I/I) [1], Vapor phase doping (VPD) or plasma doping [2] etc.,. Adequate development of these processes depends on the ability to observe the resulting 3D-doping profiling techniques with nanometer precision. The latter emphasizes the need for metrology tools that can probe dopants in 3D with nm-resolution.

In this work we have developed a methodology based on the APT [3] to probe the 3D-dopant distribution inside a FinFET device and extract the important parameters such as gate overlap and profile gradient. The FinFET devices used in this work originate from a standard process flow whereby the doping step is based on a plasma doping concept and with traditional beam-line ion implants (I/I). The extracted dopant profiles are then correlated with device performance.

Device fabrication and Sample preparation: The test structures for the extraction of the 3D dopant profiles, consist of repeated arrays of 5 parallel fins with a Fin height (H_{fin}) around 60nm and a Fin width (W_{fin}) around 40nm. After Fins etching a gate is formed consisting of ~5nm TiN and ~2nm HfO₂. The source/drain (S/D) regions of fins were doped with Arsenic by using standard 2 Quad I/I with either 10° & 45° tilt or with two different plasma doping processes (termed A, B hereafter). To facilitate the APT analysis the entire structures are then covered with (~100 nm) poly silicon. Fig. 1 shows the SEM image of the 3D structures after gate patterning, plasma doping (plasma-A) and spike annealing.

The sample preparation is a crucial step to perform APT analysis. APT uses the principle of electrical field evaporation to remove the atoms from the sample by a high electrical field, typically 30-100 V/nm. In order to achieve the required field strength the sample needs to be structured in the shape of a needle with radius ~10-100nm as the applied field can be approximated by $F=V/R$ (with 'V' applied voltage, 'R' radius of the sample). The sample preparation is performed by Focused Ion Beam (FIB) whereby e-beam deposited platinum and FIB marking are used to protect the area of interest from the Ga-interactions and to identify the region of interest [4]. The entire process is completed with a Lift out procedure and annular milling leading to the final needle shape. In order to minimize the effect of the energetic Ga-beam, the Ga-energy is gradually reduced from 30kV to 2kV during the annular milling. [3].

Results and Discussion: Fig. 2, 3 & 4 illustrate that the 3D-distribution of atoms from the S/D to 3D-gate stack regions, as obtained on a complete 3D-Fin transistor. Fig. 2 shows the 2D-As-distribution obtained with APT in S/D region. Fig. 3 shows a cross section view along the fin illustrating the diffused dopant profile from S/D to Gate. Fig. 4 shows the 2D-distribution of Arsenic atoms under the spacer at the gate edge and S/D region. Plasma-A clearly leads to a much higher doping at the top of the Fin as compared to the sidewall and is thus highly non-conformal (cfr also fig.5 and table 1). The higher doping at the top then induces a larger under diffusion and thus larger gate overlap at the top of the fin versus the sidewall (cfr Fig.3).

From the 3D-distributions we extract the lateral and vertical dopant profiles in the S/D region and their in-diffusion after anneal (Fig.5). Similarly we show in Fig.6 the profiles from S/D region to Channel, taken near the top of the Fin top (in center of the fin width) and near the bottom of the fin. The as-doped profiles show a lateral in-diffusion gradient ~3-4 nm/decade slightly steeper than the vertical in-diffusion gradients (fig. 5 & 6). After annealing the lowly doped part of the sidewall shows a small increase up to a 7-8 nm/decade gradient similar to the profiles observed at side wall in S/D region (fig 5). However in the top part of the Fin the profile develops a very different shape, characterized by a slope of 15 nm/decade ending eventually with a much steeper section of ~7-8 nm/decade. Defining the lateral junction depth (Gate overlap) at a level of 1×10^{19} at/cm³ the junction depth increases from 2 to 7 nm (bottom) and 10 to 25 nm (top) upon the anneal.

In order to assess the efficiency of the various doping processes we compare in Fig.7 the lateral distribution of Arsenic (Orange) within the native oxide (Green) at the sidewalls of the fin, for I/I (at 10° and 45° tilt) and Plasma (A, B) in the S/D regions. Obviously a small tilt angle leads to a poor sidewall doping which can be improved by going to a 45° tilt or an optimized plasma (B) doping step. Similarly Fig. 8 & 9 show the comparison of the Lateral (at mid sidewall) and Vertical (top) dopant profiles for each case. From fig.9 it is clear that plasma-A has a much higher peak concentration and dose at the top of fin as compared to I/I and plasma-B. Based on the sidewall profiles (Fig.8) we can extract the dose conformalities as obtained by APT (Table 1). The vertical (top) and lateral junction depths values are summarized in Table 2.

When comparing the results of table 1 with actual device performance, it is clear that side wall dose is the dominant factor as plasma-B with the highest side wall dose (Fig.8) also has the highest device performance (Fig.10) [5]. Vice versa plasma-A has a high top dose but a low side wall dose leading to a poor device performance. When comparing the active dopant concentration (as can be extracted from resistors) and with the non-active (APT) average dopant concentration (Fig.11) it is clear that for all the cases the degree of conformality is higher when looking at the active dopant concentration. This can be explained by the fact that through dopant clustering [6] and segregation not all dopants are active in the highly doped (top) regions whereas in the side wall the lower concentrations lead to a higher activation.

Conclusions: A methodology for the complete analysis of the 3D-dopant distribution has been developed based on APT. Precise dopant distributions within a fin have been resolved enabling to link the process optimization with device performance.

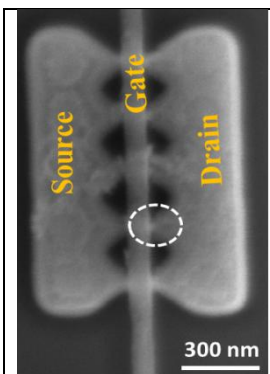


Figure 1: SEM image of structure prior to the poly silicon deposition. The circled location is the area of the interest for APT analysis.

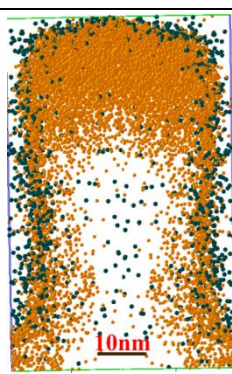


Figure 2: APT image of Arsenic (orange) and oxide (SiO₂, green) at top and side wall of the fin in S/D region.

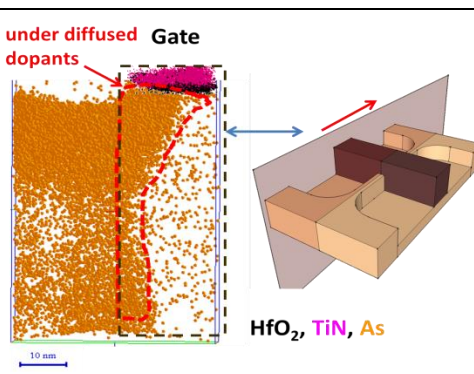


Figure 3: APT atomic map of Arsenic doping & diffusion from S/D region to Gate (see the Schematic). Silicon atoms are not shown, Orange -> As, Black -> HfO₂, Pink-> TiN. The Red dotted line shows under diffused dopant distribution into the channel under the Gate.

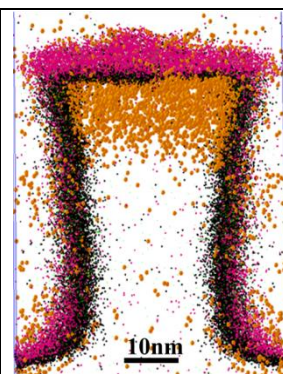


Figure 4: APT analysis of As dopants at the gate and S/D interface, (Orange) and gate stack composed of HfO₂ (black) and TiN (Pink).

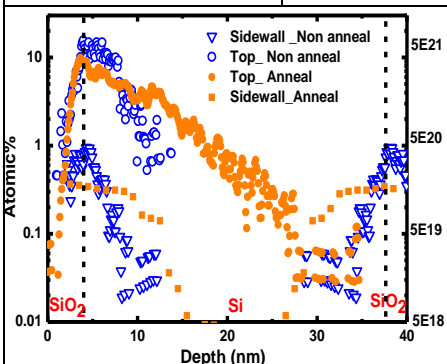


Figure 5: Vertical dopant profiles extracted at sidewall and Top of the Fin in Source/Drain region before and after anneal.

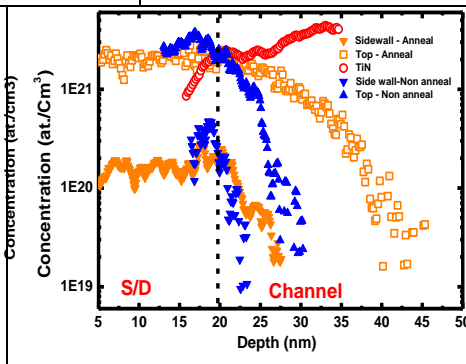


Figure 6: Lateral (Gate overlap) profiles from S/D region to Gate region for Annealed and Non-Annealed samples at top and bottom of sidewall. The TiN (red) line marks the gate edge

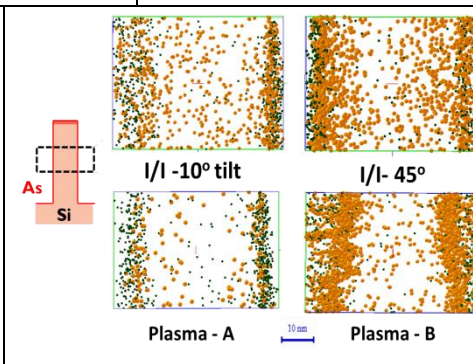


Figure 7: Lateral Arsenic dopant distribution at S/D regions for I/I (10° and 45° tilt) and Plasma processes. (Green -> SiO₂, Orange -> As).

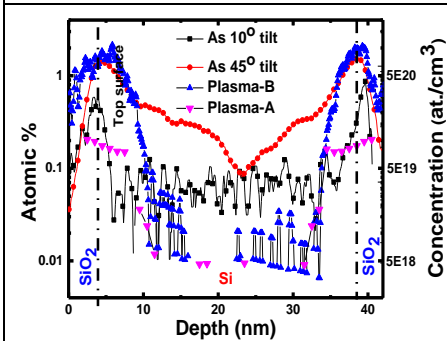


Figure 8: Lateral dopant profiles in S/D region for I/I and Plasma processes.

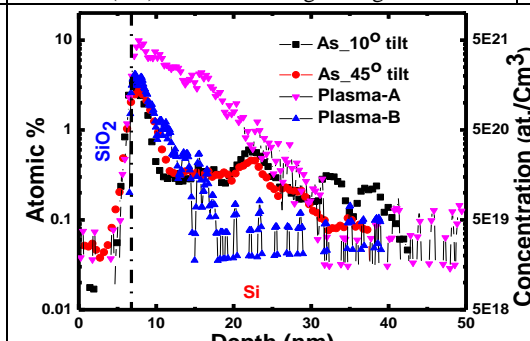


Figure 9: Vertical dopant profiles for I/I and Plasma processes taken in center of Fin at S/D region.

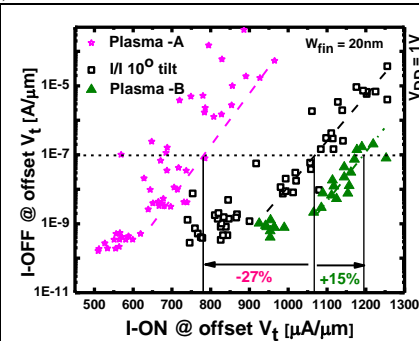


Figure 10: Device Performance for I/I and plasma processes

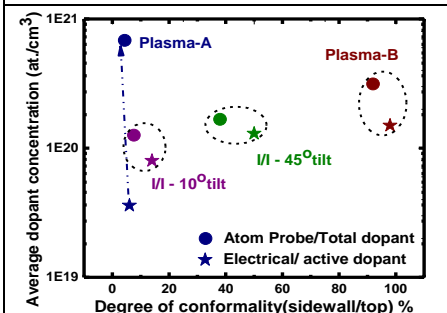


Figure 11: Comparison of conformality vs. average concentration extracted from APT and electrical analysis (resistors).

Process	Single side wall (Ions/cm ²)	Fin top dose (Ions/cm ²)	(Side wall/ Top)%
Plasma- A	1.57x 10 ¹⁴	35.4x 10 ¹⁴	4.4
I/I - 10°	0.7 x 10 ¹⁴	9.2x 10 ¹⁴	7.6
I/I - 45°	3.15 x 10 ¹⁴	8.2 x 10 ¹⁴	38
Plasma -B	6.5x 10 ¹⁴	7x 10 ¹⁴	93

Table 1: Dopant dose and conformality by APT.

Process	X _V	X _L
I/I-10°	~25	~5
I/I-45°	~25	~20
Plasma-A	~25	~6
Plasma-B	~14	~12

Table 2: Vertical (X_V) and Lateral (X_L) Junction depths for I/I and plasma processes.

- References:** 1. R. Duffy et al, J. Vac. Sci. Technol. B 26(1), pp. 402 – 407, 2008. 2. Y. Sasaki et al, IEDM Tech. Digest, pp. 917-920, 2008. 3. A.K. Kambham et al, Ultramicroscopy 111(6), 535-539 (2011). 4. A.K. Kambham et al, <http://dx.doi.org/10.1016/j.ultramic.2012.09.013>. 5. G Zschaetzsch et al., IEDM Tech. Digest, pp. 841-843, 2011. 6. A.K. Kambham et al, Nanotechnology 24 (2013) 275705.